DOI: 10.1002/ejic.201001026

A First TDDFT Study of Metallocorrole Electronic Spectra: Copper *meso*-Triarylcorroles Exhibit *Hyper* Spectra

Abraham Alemayehu,[a] Jeanet Conradie,*[a,b] and Abhik Ghosh*[a]

Keywords: Corroles / Density functional calculations / Substituent effects / Copper / Silver

The Soret maxima of a number of metallotriarylcorrole derivatives, notably the copper corroles, are exquisitely sensitive to substitutions on the *meso* phenyl groups. In contrast, the Soret maxima of silver triarylcorroles are essentially invariant with respect to phenyl-group substituents. TDDFT calculations indicate that the substituent sensitivity in the copper case results from significant phenyl-to-metal charge-transfer character in the main peaks of the Soret region. In other words, copper triarylcorroles exhibit so-called *hyper* spectra. By contrast, the Soret region in the silver case is largely $\pi \rightarrow \pi^*$ in nature. DFT calculations suggest that the difference in nature of the Soret bands reflects the energy difference between the LUMOs of the copper and silver complexes, which, in both cases, may be described as an antibonding metal-($d_{x^2-y^2}$)-corrole(π)-based MO. Strong support for this picture comes from electrochemistry: the reduction potentials of silver triarylcorroles are about 0.7–0.8 V more negative than for the analogous copper complexes. In the same vein, the "electrochemical HOMO–LUMO gaps" are ca. 1 eV for the silver corroles and only 0.8 eV for their copper analogues.

Introduction

Peripheral substituents bring about striking shifts in the electronic absorption spectra of certain transition-metal corroles.[1,2] These are all the more remarkable because similar substituent effects are not observed for the analogous metalloporphyrins. Thus, the Soret maxima of copper, manganese, and iron *meso*-triarylcorroles all red-shift significantly with the attachment of electron-donating substituents on the *meso*-phenyl groups.[2] This behavior may be contrasted with that of nickel or copper tetraarylporphyrins, whose electronic spectra are relatively insensitive to substitutions on the *meso*-phenyl groups. Free-base and closed-shell diboron[3] triarylcorroles also do not exhibit much by way of substituent-induced shifts. The simplest explanation for these phenomena appears to be that the Soret regions of metallocorroles have significant charge-transfer (CT) character, a reasonable suggestion in view of the overall high-valent nature of most transition-metal corroles.[2,4]

With today's computational technology, it would appear to be a simple matter to unravel the phenomena described above and to assign the electronic spectra of metallocorroles.[5,6] In practice, however, the matter is not quite so simple. First, the performance of time-dependent density functional theory calculations, currently the obvious first choice for calculations of electronic absorption spectra, for high-valent, potentially noninnocent systems such as metallocorroles is unknown. Second, the ground states of certain metallocorroles exhibit broken-symmetry character, i.e. significant spatial separation of α- and β spin densities;[7] these provide questionable starting points for TDDFT calculations. Under the circumstances, we have adopted a combination of experimental and theoretical approaches to obtain a better understanding of metallocorrole electronic spectra.

In a first major TDDFT exploration of metallocorroles, we have examined two series of complexes, viz. Cu and Ag[8] *meso*-triarylcorroles (Scheme 1) with varying *para* substituents on the *meso* phenyl groups, henceforth symbolized M[T(*p*-X-P)C], where M = Cu and Ag and X = CF_3, H, CH_3, and OCH_3.[9] For both series of complexes, DFT calculations with pure exchange-correlation functionals (albeit not necessarily with hybrid functionals) result in fully spin-

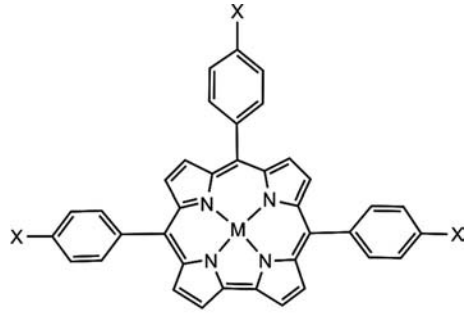

M = Cu, Ag
X = CF_3, H, CH_3, OCH_3

Scheme 1.

[a] Department of Chemistry and Center for Theoretical and Computational Chemistry,
University of Tromsø, 9037 Tromsø, Norway
E-mail: conradj@ufs.ac.za
abhik.ghosh@uit.no
[b] Department of Chemistry, University of the Free State, 9300 Bloemfontein, Republic of South Africa

Supporting information for this article is available on the WWW under http://dx.doi.org/10.1002/ejic.201001026.

paired (i.e. not broken-symmetry) descriptions, which provide a legitimate starting point for TDDFT calculations. The results provide not only a number of significant insights into metallocorrole electronic absorption spectra but also a critical assessment of the performance of TDDFT, including some of its pitfalls.

Results and Discussion

The electronic absorption spectra of Cu and Ag *meso*-triarylcorroles that we seek to model are shown in Figure 1. Selected redox potentials are listed in Table 1 and cyclic voltammograms (CVs) of the Ag derivatives are shown in Figure 2; the CVs of the copper triarylcorroles have already been reported in an earlier paper.[2a]

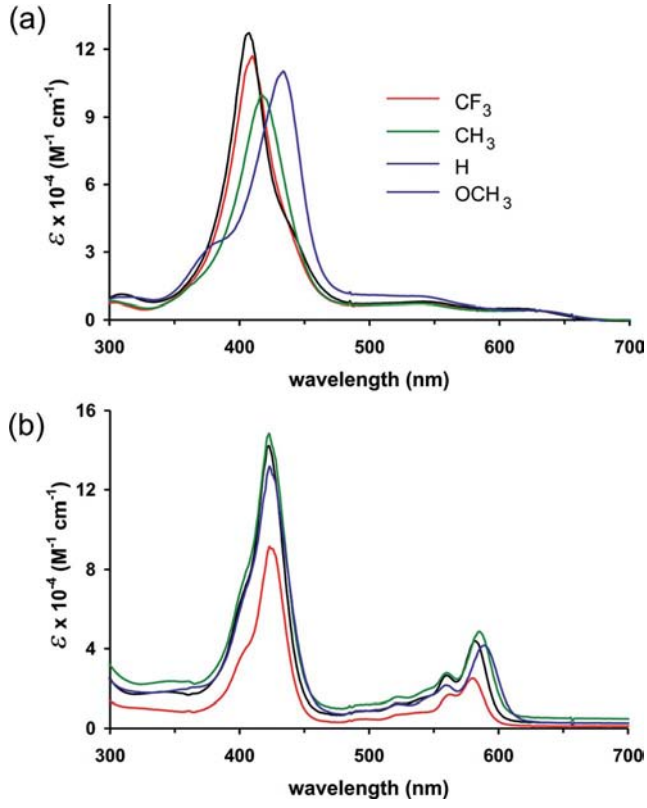

Figure 1. Electronic absorption spectra of (a) Cu[T(*p*-X-P)C] and (b) Ag[T(*p*-X-P)C] in CH_2Cl_2.

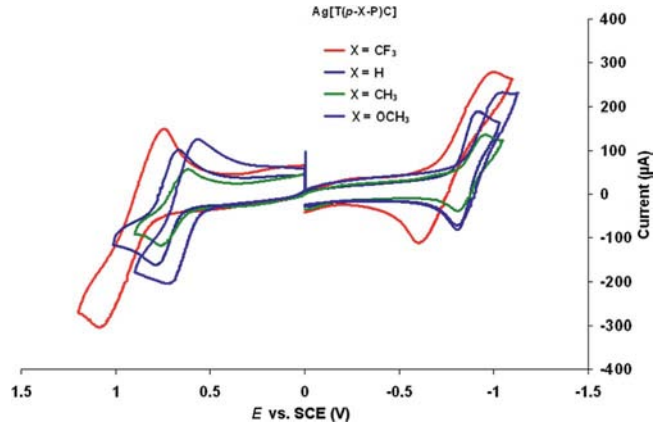

Figure 2. Cyclic voltammograms of Ag[T(*p*-X-P)C] in CH_2Cl_2 (see Supporting Information for experimental details).

The Parent Chromophores, Cu(TPC) and Ag(TPC)

Table 2 presents a detailed description (OLYP[10]/STO-TZP) of the two main Soret transitions of the two "parent" complexes. Figure 3 depicts the energy levels of the frontier MOs, and Figure 4 illustrates the MOs themselves. The qualitative shapes of the frontier MOs are nearly identical for the Cu and Ag complexes; the energy levels, especially the LUMO level and HOMO–LUMO gap, however, are somewhat different, as discussed below.

Before discussing the results, however, we need to point out a key structural feature of copper and silver corroles, viz. a certain inherent saddling (i.e. the pyrrole rings are alternately tilted up and down relative to the mean plane of the macrocycle), which is dictated by a metal($d_{x^2-y^2}$)–corrole(π) orbital interaction.[11] The corrole π orbital in question is the porphyrin a_{2u}-like π HOMO; saddling allows this π MO to overlap with the metal $d_{x^2-y^2}$ orbital. This overlap may be seen from the topologies of both the HOMO and the LUMO of Cu(TPC) (Figure 4). One might naively expect that the metal–corrole interaction should be overall bonding in the HOMO and overall antibonding in the LUMO, which, however, is not seen in Figure 4: both MOs show a net metal–corrole antibonding interaction. The reason is that both MOs involve mixing with yet a third orbital, viz. a nitrogen lone-pair-based MO that transforms as b_{1g} in a D_{4h} porphyrin. The MO where *both* the corrole

Table 1. Half-wave potentials ($E_{1/2}$, V vs. SCE, in CH_2Cl_2 containing 0.1 M TBAP) and Hammett analysis results for Ag and Cu *meso*-triarylcorroles. The combined σ and σ^+ constants for the three *para* substituents are listed for each complex. Hammett ρ and ρ^+ [mV, defined as $(1/3)\cdot d(E_{1/2})/d\sigma$] are indicated for each series of metallocorroles, along with the R^2 values for each plot (in italics within parentheses).

M	X	3σ	$3\sigma^+$	$E_{1/2(ox)}$	$E_{1/2(red)}$	ρ_{ox}	ρ^+_{ox}	ρ_{red}	ρ^+_{red}
Ag	CF_3	1.62	1.836	0.91	–0.78	104	60.6	51	31.1
	H	0.00	0.000	0.73	–0.86	(0.997)	(0.893)	(0.987)	(0.959)
	CH_3	–0.51	–0.933	0.69	–0.88				
	OCH_3	–0.80	–2.334	0.66	–0.91				
Cu	CF_3	1.62	1.836	0.89	–0.08	95	58.5	68	39.2
	H	0.00	0.000	0.76	–0.20	(0.979)	(0.976)	(0.993)	(0.865)
	CH_3	–0.51	–0.933	0.70	–0.23				
	OCH_3	–0.80	–2.334	0.65	–0.24				

Table 2. TDDFT (OLYPTZP) results for the main Soret transitions for Ag(TPC) and Cu(TPC): energies (*E*, eV), state symmetry (A or B) and oscillator strength (*f*).

E (eV)	Symmetry	λ (nm)	*f*	From	To	% Contribution
Ag(TPC), optimized with $\chi_1 = \chi_2 = \chi_3 = 0°$						
2.94008	A	422	0.3936	HOMO	LUMO+2	45.7
				HOMO-1	LUMO+1	31.5
				HOMO-2	LUMO+1	11.5
				HOMO-16	LUMO	5.1
2.96776	B	418	0.4743	HOMO-1	LUMO+2	70.0
				HOMO	LUMO+1	15.8
				HOMO-15	LUMO	4.7
Ag(TPC), optimized with $\chi_1 = \chi_2 = \chi_3 = 25°$						
2.8492	A	435	0.2977	HOMO	LUMO+2	24.3
				HOMO-1	LUMO+1	21.1
				HOMO-8	LUMO	15.2
				HOMO-6	LUMO	9.8
				HOMO-12	LUMO	7.9
				HOMO-2	LUMO+1	5.8
2.8859	B	430	0.6006	HOMO-1	LUMO+2	60.5
				HOMO	LUMO+1	13.2
				HOMO-5	LUMO	7.3
Ag(TPC), fully optimized						
2.876	A	431	0.2598	HOMO-6	LUMO	28.4
				HOMO	LUMO+2	17.5
				HOMO-11	LUMO	15.4
				HOMO-1	LUMO+1	15.3
				HOMO-12	LUMO	5.6
				HOMO-2	LUMO+1	5.3
				HOMO-3	LUMO	3.7
				HOMO-7	LUMO	2.7
2.878	B	431	0.4792	HOMO-1	LUMO+2	40.1
				HOMO-5	LUMO	18.4
				HOMO-9	LUMO	12.2
				HOMO	LUMO+1	10.2
				HOMO-10	LUMO	3.9
				HOMO-14	LUMO	3.4
				HOMO-2	LUMO	3.4
Cu(TPC), fully optimized						
2.798	A	443	0.2333	HOMO-12	LUMO	34.1
				HOMO	LUMO+2	24.5
				HOMO-1	LUMO+1	18.5
				HOMO-6	LUMO	10.8
				HOMO-2	LUMO+1	2.4
				HOMO-10	LUMO	2.2
2.831	B	438	0.5006	HOMO-1	LUMO+2	53.3
				HOMO	LUMO+1	11.9
				HOMO-13	LUMO	11.9
				HOMO-5	LUMO	8.3
				HOMO-15	LUMO	5.9

"a_{2u}" and the N "b_{1g}" orbitals engage in a bonding interaction with the metal $d_{x^2-y^2}$ orbital is much lower in energy, i.e. does not rank among the frontier MOs.

Saddling is a rather soft mode, and we have observed that, although DFT optimizations appear to accurately reproduce the saddling of copper corroles, relatively little is known experimentally about the conformational preferences of silver corroles. To date, the crystal structure of only one silver *meso*-triarylcorrole, Ag(TPC),[8a] has been reported, and it shows saddling dihedrals averaging about

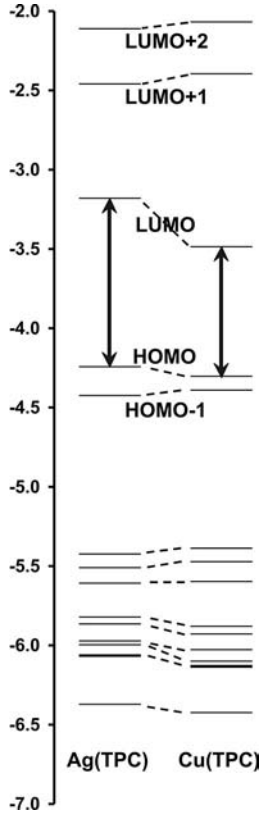

Figure 3. OLYP/TZP MO Kohn–Sham energy [eV] levels for Ag(TPC) and Cu(TPC). For constructing this diagram (but not elsewhere in the paper unless stated), we have assumed C_2 symmetry. The *y* axis denotes relative energy in eV.

40°, similar to or slightly lower than that commonly observed for copper triarylcorroles. To obtain a better idea of the influence of saddling on the electronic spectra, we obtained a number of partially constrained, C_2 optimized structures of Ag triarylcorroles with fixed saddling dihedrals (χ_1–χ_3), these being defined in Scheme 2.

The TDDFT calculations, as summarized in Table 2, provide major insights into the Soret region of Cu and Ag triarylcorroles. First and foremost, they clearly show that the main Soret transitions of Cu(TPC) have a large charge-transfer component. Slightly under 50% of the major A-symmetry Soret feature at 2.798 eV (see Table 2) involves excitations from the phenyl-based MOs HOMO-12 (34%) and HOMO-6 (11%) into the LUMO, which is about a third Cu $d_{x^2-y^2}$ in character. The major B-symmetry Soret feature has substantially lower, but still significant, phenyl-to-Cu charge-transfer character. In our early DFT studies to understand Cu corrole electronic spectra carried out nearly a decade ago, we had correctly appreciated the importance of the Cu($d_{x^2-y^2}$)-based LUMO, but had not accounted for the phenyl groups in our models.[2a,12] Applying Gouterman's classification of porphyrin spectra to corroles, we may say that copper corroles exhibit *hyper* spectra.[13,14]

The Soret transitions of Ag(TPC), by contrast, show significantly less phenyl-to-LUMO CT character, especially for low saddling dihedrals. The lower CT character of the main

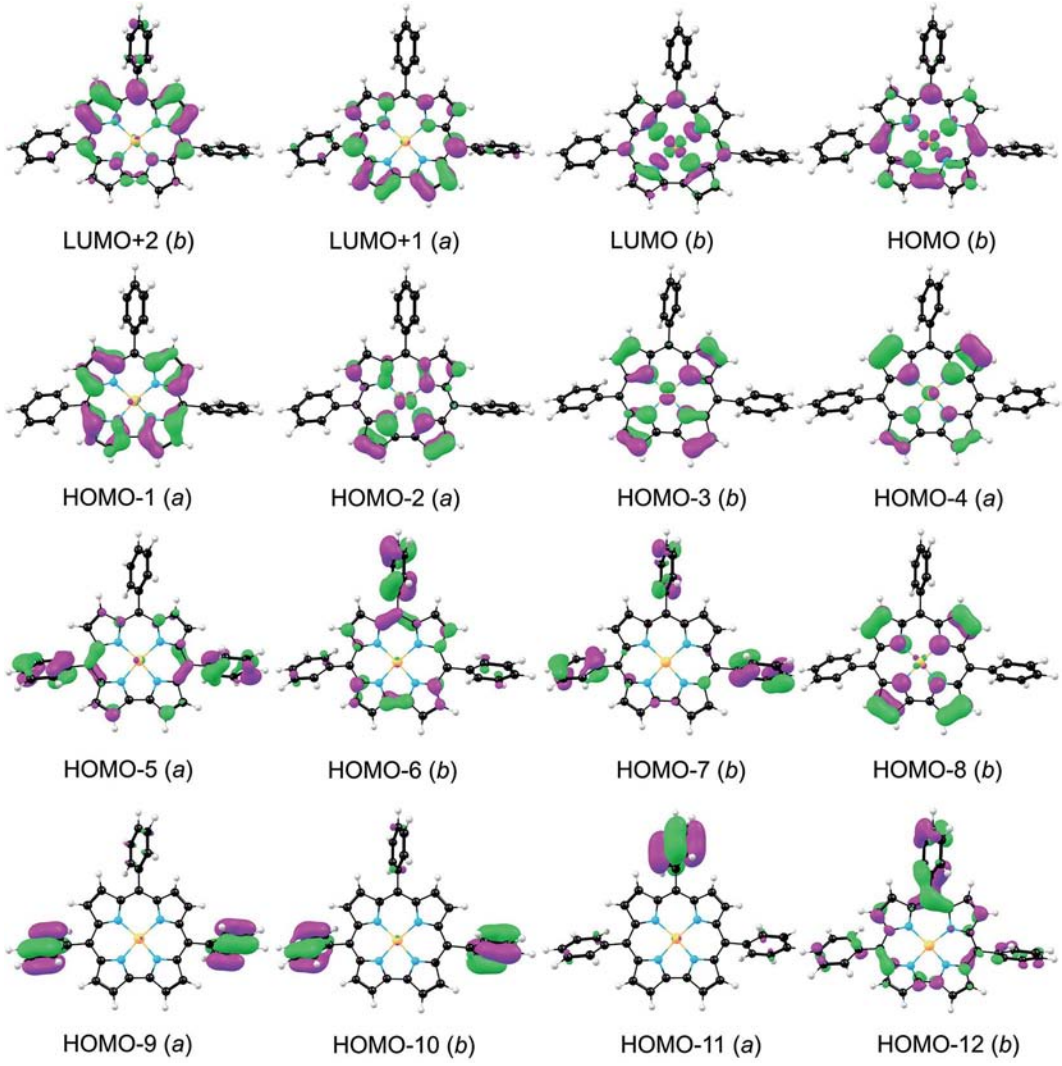

Figure 4. Frontier MOs, with their C_2 irreps (irreducible representations, a or b), for Cu(TPC). The qualitative shapes of the frontier MOs, as well as their energy ordering, are essentially the same for Ag(TPC).

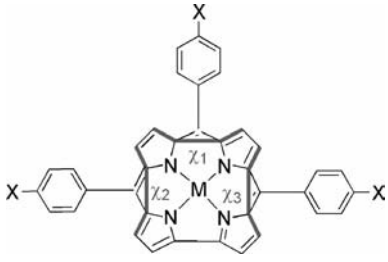

Scheme 2.

Soret transitions is *qualitatively* consistent with the observed lack of substituent effects on the Soret maximum of silver *meso*-triarylcorroles. Table 2 also shows the importance of saddling on the proportion of CT character in the Soret transitions.

Substituent Effects

Table 3 presents experimental and calculated Soret maxima for the various M[T(*p*-X-P)C] complexes studied. Figure 5 presents artificial spectra in which Gaussians with FWHMs of 30 nm are used to broaden the TDDFT features. As the *para* substituents become increasingly electron releasing, the experimental Soret maxima of the Cu derivatives redshift markedly, but those of the Ag derivatives remain essentially unchanged. The capturing of these substituent effects faithfully constitutes a stringent test for TDDFT (or, for that matter, for any excited-state quantum chemical methodology).

The performance of TDDFT with regard to these substituent effects is rather mixed. TDDFT does a fair job of capturing the Soret redshift on addition of methyl groups on the *meso*-phenyl substituents of Cu(TPC). For Ag[T(*p*-CH_3-P)C], the calculated redshifts are somewhat lower than those for Cu[T(*p*-CH_3-P)C], which is qualitatively consistent with the experimental scenario. However, the variation in the Soret maximum with the degree of saddling makes a detailed comparison with experiments somewhat tricky.

On the other hand, the TDDFT simulated spectra of the T(*p*-CF_3-P)C and T(*p*-OCH_3-P)C are clearly unsatisfactory,

Table 3. Experimental (in CH_2Cl_2) and calculated Soret maxima [nm] of triarylcorrole derivatives.

Corrole	Geometry/Details	CF_3	H	CH_3	OCH_3
Ag[T(*p*-X-P)C]	experimental	423	423	423	423
	optimized, with $\chi_1 = \chi_2 = \chi_3 = 0°$	423, 415	422, 418	422, 418	418, 425
	optimized, with $\chi_1 = \chi_2 = \chi_3 = 25°$	468, 465, 439, 438	435, 430	442, 435, 433	456, 442
	fully optimized	464, 462, 427, 425	431, 431	434, 433	453, 443, 441
Cu[T(*p*-X-P)C]	experimental	407	413	418	433
	fully optimized	449, 448	443, 438	454, 445	467, 453

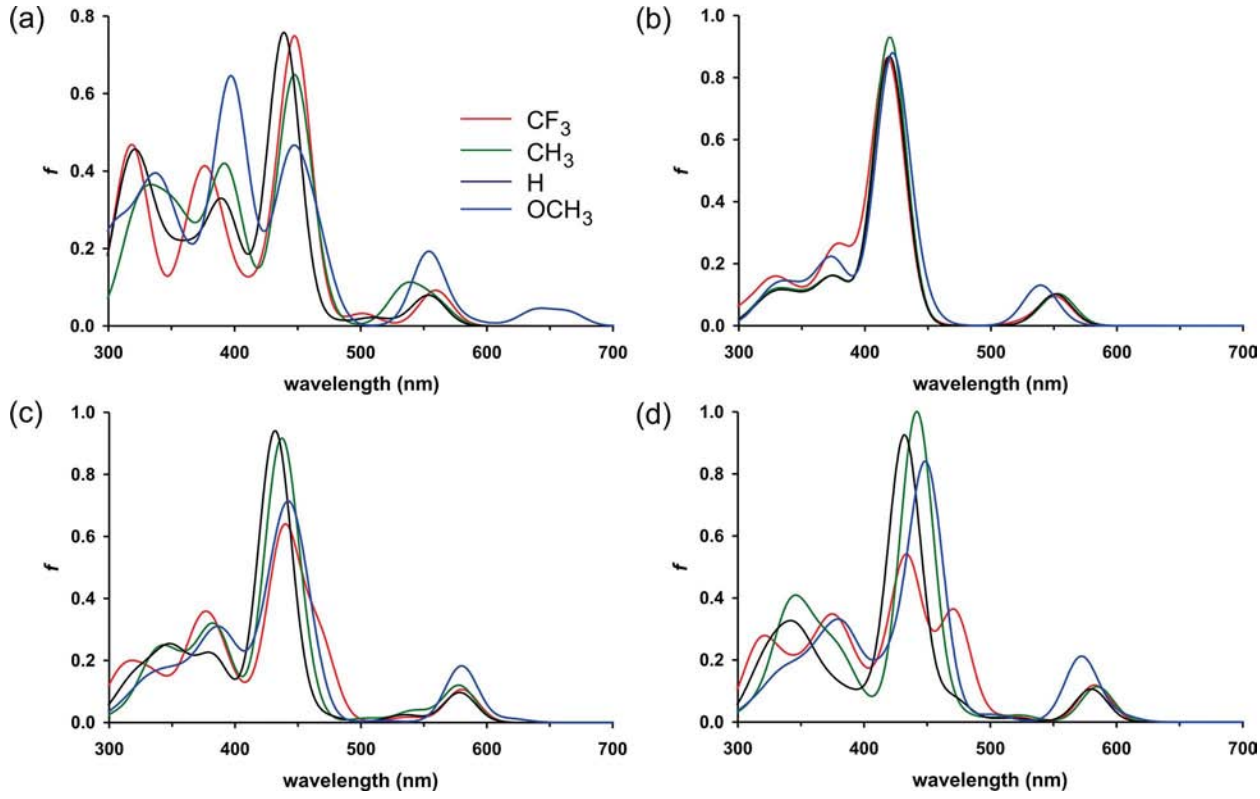

Figure 5. Artificial TDDFT-based electronic absorption spectra of (a) Cu[T(p-X-P)C] and Ag[T(p-X-P)C] with dihedrals fixed at (b) 0°, (c) 25° and (d) 50°. The artificial spectrum has been generated by broadening the lines with Gaussian functions with a band half-width of 30 nm.

i.e. they are affected by undesirable artifacts. Thus, for Cu[T(*p*-OCH_3-P)C] (see Figure 5), TDDFT predicts an intense "N band" centered around 400 nm, at a higher energy relative to the main Soret feature. The experimental spectrum (Figure 1) does show a significant higher-energy shoulder on the Soret band; however, the calculated intensity of the 400-nm feature is disproportionately high, relative to the experimental results.

For Ag[T(*p*-CF_3-P)C] (see Figure 5), TDDFT predicts a substantial shoulder or peak to the red of the main Soret feature. No comparable feature occurs in the experimental spectrum, although experimentally all the silver corroles do exhibit a significant shoulder on the higher-energy side of the main Soret peak.

The rather voluminous body of TDDFT data on all these compounds does not warrant a detailed discussion. However, the intense, nonphysical peaks appear to arise from CT out of the lone pairs of the CF_3 and OCH_3 substituents. These last findings confirm one of TDDFT's known deficiencies, viz. it generally does not provide a good description of long-range CT transitions.[15]

A Note on Solvent Effects

Table 4 presents experimental Soret maxima for the various Cu[T(*p*-X-P)C] complexes studied in a variety of solvents. Figure 6 presents the calculated artificial spectra of Cu(TPC) and Ag(TPC) in selected solvents calculated with the conductor-like screening model (COSMO). Gaussians with FWHMs of 30 nm were used to broaden the TDDFT features.

Charge-transfer absorption features often shift sensitively as a function of the solvent – they are generally redshifted in more polar solvents, as the CT state becomes more stabilized. For the Cu(TPC) derivatives, however, such solvent

Table 4. Experimental Soret maxima [nm] of Cu[T(*p*-X-P)C] derivatives recorded in various solvents at room temperature (X = CF_3, H, CH_3 and OCH_3).

Solvent	ε	$\lambda(CF_3)$	λ(H)	$\lambda(CH_3)$	$\lambda(OCH_3)$
n-hexane	1.88	405	405	412	428
toluene	2.38	411	412	419	435
tetrahydrofuran	7.85	408	409	416	433
dichloromethane	8.9	407	410	418	434
methanol	32.6	403	405	414	429
dimethylformamide	37.0	409	411	420	435
acetonitrile	37.5	404	406	411	431
dimethylsulfoxide	46.7	416, 440	414	423	437

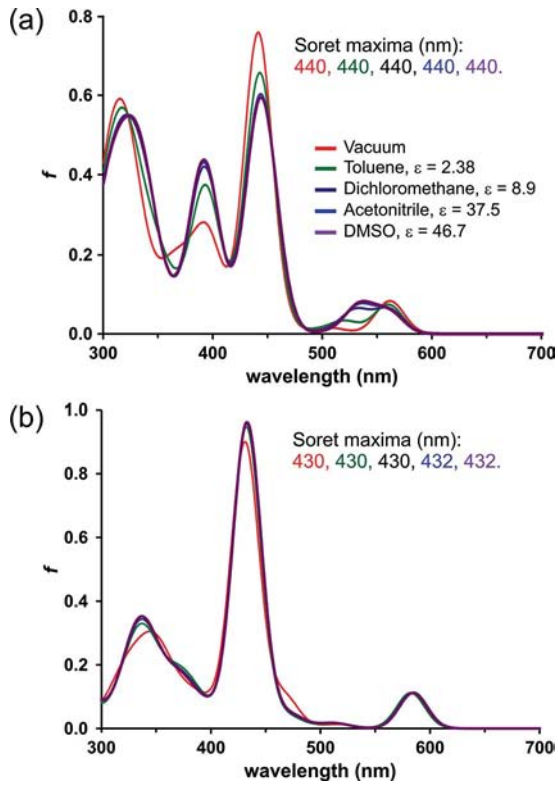

Figure 6. Artificial TDDFT-based electronic absorption spectra of (a) Cu(TPC) and (b) Ag(TPC), calculated for various solvents with the COSMO model. The artificial spectra have been generated by broadening the lines with Gaussian functions with band half-widths of 30 nm.

shifts are rather small (up to 9 cm^{-1}) and indeed somewhat erratic. A plausible reason is that the charge transfer in question involves a migration of electron density from the periphery of the molecule (the phenyl groups) to the center (i.e. the copper atom) and is not accompanied by the creation of a large dipole moment, such as would occur for a relatively linear donor–acceptor assembly. TDDFT calculations on Cu(TPC) and Ag(TPC) are consonant with our experimental observations and do not evince any major solvent effects either.

Copper vs. Silver

The mixed performance of TDDFT led us to seek alternative approaches to rationalizing the differences in substituent effects between copper and silver triarylcorroles. An examination of the Kohn–Sham orbital energy levels for the different Cu and Ag complexes (Figure 7) did not prove particularly illuminating. The substituent effects on individual orbital energies are nearly identical for both metals, which is not surprising. Although we have not carried out explicit calculations of redox potentials in this project, it is satisfying to note that the substituent effects on the HOMO and LUMO of these complexes are in good qualitative accord with electrochemical data (Table 1).

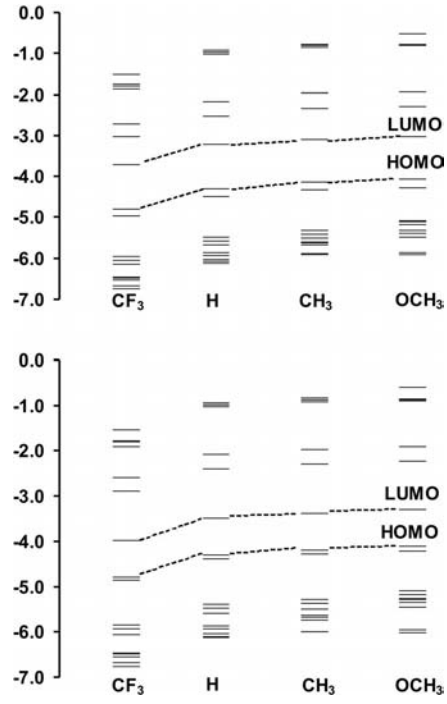

Figure 7. OLYP/TZP Kohn–Sham energy levels [eV] for Ag[T(*p*-X-P)C] (top) and Cu[T(*p*-X-P)C] (bottom).

Perhaps the most important clue provided by the Kohn–Sham orbital energies is that the silver corroles have higher-energy LUMOs relative to their copper analogues, as well as higher HOMO–LUMO gaps. Although this is qualitatively consistent with a lesser degree of CT character in the Soret region of the silver corroles, the copper and silver energy levels differ by only about 0.2–0.3 eV; such a minor difference does not appear to be sufficient to account for the observed difference in substituent effects between the two metal complexes.

Fortunately, electrochemical data appear to suggest a plausible explanation for this conundrum. As shown in Table 1, the reduction potentials of the Ag triarylcorroles are about 0.7 V lower than those of their Cu analogues (see Table 1). The "electrochemical HOMO–LUMO gaps" (the difference between oxidation and reduction potentials) are also very different – about 1.6 eV in the Ag case vs. only 0.8 eV in the Cu case, i.e. far more different than the Kohn–Sham HOMO–LUMO gaps. A difference in this magnitude in the LUMO energies and in the HOMO–LUMO gaps is certainly sufficient to account for significant LMCT (or *hyper*[14]) character in the Soret region of Cu corroles, but not

for their Ag analogues. In turn, this also provides a qualitative explanation for the strong substituent effects on the Soret maxima of Cu corroles and for the lack of such effects in Ag corroles.

Conclusions

We have carried out a first TDDFT analysis of metallocorrole electronic spectra. Despite significant limitations, the TDDFT calculations yield a number of important insights, our main conclusions being as follows.

Copper triarylcorroles exhibit so-called hyper spectra; the Soret band includes one or more transitions with substantial phenyl-to-Cu($d_{x^2-y^2}$) charge-transfer character. Although the LUMO of copper corroles has long been recognized as having substantial Cu($d_{x^2-y^2}$) character, this is the first time that the importance of the *meso*-aryl groups vis-à-vis the Soret band has been analyzed.

Silver corroles, not surprisingly, have an MO structure that is similar to that of copper corroles. However, there is comparatively little charge-transfer character in the Soret transitions of silver corroles, at least for small amounts of saddling. Electrochemical data suggest that the difference in substituent effects between the Cu and Ag cases appears to be related to a much higher energy LUMO and a much larger HOMO–LUMO gap in the silver case.

The TDDFT calculations do a fair job of reproducing the Soret redshift of Cu[T(*p*-CH_3-P)C] relative to that for Cu(TPC). The calculations, however, do not provide a good description of the Soret region of the *p*-CF_3 and *p*-OCH_3 derivatives. Overall, it appears that for the parent TPC derivatives, as well as for the T(*p*-CH_3-P)C complexes, the metal, corrole, and phenyl orbitals are all sufficiently mixed that the entire molecule behaves as a single chromophore, which leads to good performance by TDDFT. This feature breaks down with the introduction of lone-pair–containing substituents such as CF_3 and OCH_3 on the phenyl groups; TDDFT leads to nonphysical, strong transitions arising from excitations out of the lone pairs of these substituents.

Interestingly, in contrast to the strong substituent effects, the solvent dielectric constant has only a minor and somewhat erratic effect on the position of the Soret maximum. Presumably, the Soret transition results in a movement of negative charge from the molecule's periphery toward the center, but does not result in the creation of a significant net dipole moment, as would be the case for a CT transition in a linear donor–acceptor assembly.

In future studies, we look forward to evaluating a number of other promising (but as yet less commonly used) methodologies such as DFT/CI,[16] range-separated functionals,[17] double hybrid functionals,[18] and many-body Green's function theory,[19,20] as well as even more advanced ab initio wave function methods. The capturing of substituent effects on metallocorrole electronic spectra should be a challenging objective with any of these methods.

Experimental and Computational Methods

The copper and silver derivatives studied were prepared with four different *meso*-triarylcorrole ligands. All four copper complexes and all but one silver complex are known compounds; details of the syntheses and characterization are given as Supporting Information.

The DFT calculations reported here were carried out with the OLYP exchange-correlation functional, all-electron STO-TZP basis sets, fine meshes for numerical integration of matrix elements, and suitably tight criteria for SCF and geometry optimization, all as implemented in the ADF 2009 program system.[21] Relativistic effects were accounted for the silver complexes by a ZORA Hamiltonian and ZORA basis sets (for Ag). OLYP/STO-TZP TDDFT calculations were subsequently carried out on the optimized geometries. Hybrid functionals such as B3LYP were not used on account of their propensity to give broken-symmetry electronic descriptions for these systems; as far as the ground states are concerned, we have no reason to favor either pure or hybrid functionals. Moreover, the asymptotically correct statistical average of orbital potential (SAOP[22]) method afforded no obvious advantages relative to common GGA functionals such as PW91, BP86, and OLYP, all of which performed comparably; as mentioned above, the results shown here were all obtained with the OLYP functional. Solvent effects were taken into account for selected calculations, as indicated in the text. The COSMO model of solvation[23,24,25] was used as implemented in ADF.[26] The COSMO model is a dielectric model in which the solute molecule is embedded in a molecule-shaped cavity surrounded by a dielectric medium with a given dielectric constant (ε). The type of cavity used is Esurf.[27]

Supporting Information (see footnote on the first page of this article): Experimental details, NMR spectra, MALDI-TOF spectra, and optimized Cartesian coordinates of the complexes are presented.

Acknowledgments

This work was supported by the Research Council of Norway and the South African National Research Foundation.

[1] For reviews on corroles, see: a) I. Aviv, Z. Gross, *Chem. Commun.* **2007**, 1987–1999; b) Z. Gross, H. B. Gray, *Commun. Inorg. Chem.* **2006**, *27*, 61–72.

[2] For reports on substituent effects in metallocorroles, see: a) I. H. Wasbotten, T. Wondimagegn, A. Ghosh, *J. Am. Chem. Soc.* **2002**, *124*, 8104–8116; b) E. Steene, T. Wondimagegn, A. Ghosh, *J. Phys. Chem. B* **2001**, *105*, 11406–11413; addition/correction:*J. Phys. Chem. B* **2002**, *106*, 5312–5312; c) E. Steene, T. Wondimagegn, A. Ghosh, *J. Am. Chem. Soc.* **2003**, *125*, 16300–16309; d) K. E. Thomas, I. H. Wasbotten, A. Ghosh, *Inorg. Chem.* **2008**, *47*, 10469–10478; addition/correction: K. E. Thomas, I. H. Wasbotten, A. Ghosh, *Inorg. Chem.* **2009**, *48*, 1257–1257.

[3] Z. Gross, H. B. Gray, *Comments Inorg. Chem.* **2006**, *27*, 61–72.

[4] A. M. Albrett, J. Conradie, P. D. W. Boyd, G. R. Clark, A. Ghosh, P. J. Brothers, *J. Am. Chem. Soc.* **2008**, *130*, 2888–2889.

[5] Reviews on DFT studies of porphyrins and related compounds: a) A. Ghosh, *Acc. Chem. Res.* **1998**, *31*, 189–198; b) A. Ghosh, in *The Porphyrin Handbook* (Eds.: K. M. Kadish, R. Guilard, K. M. Smith); Vol. 7 Academic: San Diego, **1999**, Ch. 47, pp. 1–38; c) A. Ghosh, E. Steene, *J. Biol. Inorg. Chem.* **2001**, *6*, 739–752; d) A. Ghosh, *J. Biol. Inorg. Chem.* **2006**, *11*, 712–724.

[6] DFT studies of corroles and corrole analogues: a) A. Ghosh, K. Jynge, *Chem. Eur. J.* **1997**, *3*, 823–833; b) A. Ghosh, T. Won-

dimagegn, A. B. J. Parusel, *J. Am. Chem. Soc.* **2000**, *122*, 5100–5104; c) J. Bendix, I. J. Dmochowski, H. B. Gray, A. Mahammed, L. Simkhovich, Z. Gross, *Angew. Chem.* **2000**, *112*, 4214; *Angew. Chem. Int. Ed.* **2000**, *39*, 4048–4051; d) E. Tangen, A. Ghosh, *J. Am. Chem. Soc.* **2002**, *124*, 8117–8121; e) B. van Oort, E. Tangen, A. Ghosh, *Eur. J. Inorg. Chem.* **2004**, 2442–2445; f) A. Ghosh, I. H. Wasbotten, W. Davis, J. C. Swarts, *Eur. J. Inorg. Chem.* **2005**, 4479–4485; g) I. Wasbotten, A. Ghosh, *Inorg. Chem.* **2006**, *45*, 4910–4913; h) A. M. Albrett, J. Conradie, A. Ghosh, P. J. Brothers, *Dalton Trans.* **2008**, 4464–4473.

[7] a) F. A. Walker, S. Licoccia, R. Paolesse, *J. Inorg. Biochem.* **2006**, *100*, 810–837; b) B. O. Roos, V. Veryazov, J. Conradie, P. R. Taylor, A. Ghosh, *J. Phys. Chem. B* **2008**, *112*, 14099–14102; c) S. Ye, T. Tuttle, E. Bill, L. Simkhovich, Z. Gross, W. Thiel, F. Neese, *Chem. Eur. J.* **2008**, *14*, 10839–10851.

[8] a) C. Brückner, C. A. Barta, R. P. Brinas, J. A. K. Bauer, *Inorg. Chem.* **2003**, *42*, 1673–1680; b) M. Stefanelli, M. Mastroianni, S. Nardis, S. Licoccia, F. R. Fronczek, K. M. Smith, W. Zhu, Z. Ou, K. M. Kadish, R. Paolesse, *Inorg. Chem.* **2007**, *46*, 10791–10799.

[9] All complexes except Ag[T(*p*-CH3-P)C] are known compounds.[2a,8] Electronic absorption spectra were measured for all the compounds studied, including those known previously. The electrochemical results, generally, are all new in this study. All experimental details are given in the Supporting Information.

[10] a) N. C. Handy, A. J. Cohen, *Mol. Phys.* **2001**, *99*, 403–412; b) C. Lee, W. Yang, R. G. Parr, *Phys. Rev. B* **1988**, *37*, 785–789.

[11] The phenomenon of inherent saddling has been discussed in two recent papers from our laboratory: a) A. Alemayehu, E. Gonzalez, L. K. Hansen, A. Ghosh, *Inorg. Chem.* **2009**, *48*, 7794–7799; b) A. Alemayehu, L. K. Hansen, A. Ghosh, *Inorg. Chem.* **2010**, *49*, 7608–7610.

[12] A. Ghosh, T. Wondimagegn, A. B. J. Parusel, *J. Am. Chem. Soc.* **2000**, *122*, 5100–5104.

[13] *Hyper* spectra are defined in: M. Gouterman in *The Porphyrins* (Eds.: D. Dolphin), Academic, New York, **1978**; vol. III, ch. 1, pp. 1–128.

[14] Selected references to hyperporphryins: a) E. C. A. Ojadi, H. Linschitz, M. Gouterman, R. I. Walter, J. S. Lindsey, R. W. Wagner, P. R. Droupadi, W. Wang, *J. Phys. Chem.* **1993**, *97*, 13192–13197; b) B. K. Manna, S. C. Bera, K. K. Rohatgi-Mukherjee, *Spectrochim. Acta Part A* **1995**, *51*, 1051–1060; c) M. Vitasovic, M. Gouterman, H. Linschitz, *J. Porphyrins Phthalocyanines* **2001**, *5*, 191–197; d) J. R. Weinkauf, S. W. Cooper, A. Schweiger, C. C. Wamser, *J. Phys. Chem. A* **2003**, *107*, 3486–3496; e) I. H. Wasbotten, J. Conradie, A. Ghosh, *J. Phys. Chem. B* **2003**, *107*, 3613–3623; f) H. Guo, J. Jiang, Y. Shi, Y. Wang, Y. Wang, S. Dong, *J. Phys. Chem. B* **2006**, *110*, 587–594; g) H. Guo, J. Jiang, Y. Shi, Y. Wang, S. Dong, *Spectrochim. Acta Part A* **2007**, *67*, 166–171.

[15] a) M. E. Casida, F. Gutierrez, J. Guan, F.-X. Gadea, D. Salahub, J.-P. Daudey, *J. Chem. Phys.* **2000**, *113*, 7062–7071; b) A. Dreuw, J. L. Weisman, M. Head-Gordon, *J. Chem. Phys.* **2003**, *119*, 2943–2946; c) A. Dreuw, M. Head-Gordon, *J. Am. Chem. Soc.* **2004**, *126*, 4007–4016.

[16] S. Grimme, M. Waletzke, *J. Chem. Phys.* **1999**, *111*, 5645–5655.

[17] For reviews, see: a) R. Baer, E. Livshits, U. Salzner, *Ann. Rev. Phys. Chem.* **2010**, *61*, 85–109; b) C. J. Cramer, D. G. Truhlar, *Phys. Chem. Chem. Phys.* **2009**, *11*, 10757–10816.

[18] a) S. Grimme, *J. Chem. Phys.* **2006**, *124*, 034108; b) S. Grimme, F. Neese, *J. Chem. Phys.* **2007**, *127*, 154116.

[19] a) G. Onida, L. Reining, A. Rubio, *Rev. Mod. Phys.* **2002**, *74*, 601–659; b) M. Rohlfing, S. G. Louie, *Phys. Rev. B* **2000**, *62*, 4927–4944.

[20] Y. Ma, M. Rohlfing, C. Molteni, *J. Chem. Theory Comput.* **2010**, *6*, 257–265.

[21] The DFT calculations were carried out with the ADF2007 program system by using methods described in: G. T. Velde, F. M. Bickelhaupt, E. J. Baerends, C. F. Guerra, S. J. A Van Gisbergen, J. G. Snijders, T. Ziegler, *J. Comput. Chem.* **2001**, *22*, 931–967.

[22] O. Gritsenko, E. J. Baerends, *J. Chem. Phys.* **2004**, *121*, 655–660.

[23] A. Klamt, G. Schüürmann, *J. Chem. Soc. Perkin Trans. 2* **1993**, 799–805.

[24] A. Klamt, *J. Phys. Chem.* **1995**, *99*, 2224–2235.

[25] A. Klamt, V. Jones, *J. Chem. Phys.* **1996**, *105*, 9972–9981.

[26] C. C. Pye, T. Ziegler, *Theor. Chem. Acc.* **1999**, *101*, 396–408.

[27] J. L. Pascual-Ahuir, E. Silla, I. Tuñon, *J. Comput. Chem.* **1994**, *15*, 1127–1138.

Received: September 27, 2010
Published Online: March 17, 2011

